Monolithically Integrated Low-Power Phototransceivers for Optoelectronic Parallel Sensing and Processing Applications

Omar Qasaimeh, *Member, IEEE*, Weidong Zhou, *Student Member, IEEE*, Pallab Bhattacharya, *Fellow, IEEE*, Diana Huffaker, *Member, IEEE*, and Dennis G. Deppe, *Fellow, IEEE*

***Abstract*—A low-power GaAs-based monolithically integrated phototransceiver, consisting of a high-gain heterojunction phototransistor (HPT) and a microcavity light-emitting diode (MCLED) or a low-threshold vertical-cavity surface-emitting laser (VCSEL), is demonstrated. The HPT and MCLED/VCSEL are grown by molecular-beam epitaxy in a single step. The phototransistor exhibits a responsivity of 60A/W at an input power of 1 μW. The input and output wavelengths are 850 and 980 nm, respectively. The MCLED-based phototransceiver exhibits an optical gain of 7dB and power dissipation of 400 μW for an input power of 1.5 μW. The small signal modulation bandwidth is 80 MHz. On the other hand, the VCSEL-based phototransceiver exhibits an optical gain of 10 dB and power dissipation of 760 μW for an input power of 2.5 μW.**

***Index Terms*—Low-power phototransciever, monolithically integrated, microcavity light-emitting diode (LED), vertical-cavity surface-emitting laser (VCSEL).**

I. Introduction

FOR optical display and image processing applications, it is necessary to develop devices and components that can detect, process, and transmit information with great adaptability and efficiency. Current image sensors are based upon high-performance, but expensive, charge-coupled devices (CCDs). The high cost of CCD-based sensors originates from the incompatibility of CCD technology with present VLSI and microelectronic technologies [1]–[4]. One way to realize affordable and easily mass-produced monolithically integrated image sensors, which could potentially affect the consumer market, involves optoelectronic parallel processing systems. Such a technology should be able to detect, process, and transmit near-perfect optical images and related information that would adapt automatically to changing scenarios and environments. A densely packed two-dimensional array of phototransceivers that can detect, process, and transmit images with high sensitivity and efficiency, and dissipate little power, would be an attractive element in current image-sensing applications. Unlike the requirements from phototransceivers in conventional optical communication systems [5]–[8], very stringent power handling and dissipation requirements have to be met. For example, in a 100×100 element array, the phototransceiver in each pixel should be capable of detecting input power as low as ~ 1 μW, and the electrical power consumption of each phototransceiver should not exceed 500 μW. Each pixel may consist of three colors (i.e., phototransceivers). The bandwidth is usually not an important factor in such massively parallel architectures.

Impressive results recently have been demonstrated in GaAs-based vertical-cavity surface-emitting lasers (VCSELs) and microcavity light-emitting diodes (MCLEDs) [9]–[17]. Threshold currents less than 40 μA and a quantum efficiency of more than 20% have been reported in oxide-confined VCSELs [9],[10], and external quantum efficiency exceeding 16% has been achieved in resonant-cavity LEDs [13]. While VCSELs are preferable in most applications, MCLEDs demonstrate higher quantum efficiency at very low injection current levels (< 40 μA). Another advantage of MCLEDs is their ease of fabrication and integration with other devices.

In this paper, we will describe the design and performance characteristics of two GaAs-based low-power phototransceiver circuits. The first circuit consists of an oxide-confined VCSEL monolithically integrated with a high-sensitivity heterojunction phototransistor (HPT). The circuit demonstrates high optical gain (10 dB) at low incident optical power (2.5 μW) and consumes relatively low electrical power (760 μW). The second circuit consists of an MCLED monolithically integrated with a high-sensitivity HPT. This circuit demonstrates an optical gain of 7 dB and dissipates 400 μW of power at $P_{\text{in}} = 1.5$ μW. In Section II, the circuit design, heterostructure growth, and fabrication steps are described. The performance characteristics of individual devices and optoelectronic integrated circuits (OEICs) are described and discussed in Section III. Finally, the most significant results are summarized in Section IV.

II. Design and Fabrication

A. Equivalent Circuit and Heterostructure Design

The phototransceiver circuit consists of a high-gain phototransistor integrated with an MCLED or an ultra-low-threshold

Manuscript received July 14, 2000; revised December 18, 2000. The work was supported by the Army Research Office (MURI program) under Grant DAAG 55-98-1-0288.

O. Qasaimeh, W. Zhou, and P. Bhattacharya are with the Department of Electrical Engineering and Computer Science, University of Michigan, Ann Arbor, MI 48105-2122 USA.

D. Huffaker and D. G. Deppe are with the Department of Electrical and Computer Engineering, The University of Texas, Austin, TX 78758-1084 USA.

Publisher Item Identifier S 0733-8724(01)02755-4.

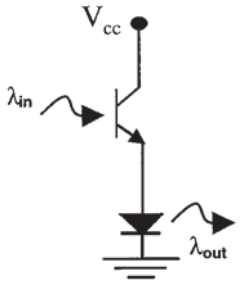

(a)

Contact Layer	GaAs 0.139μm	n^+ $3x10^{18}$ cm^{-3}
Sub-Emitter	$Al_{0.3}Ga_{0.7}As$ 894Å	N $3x10^{18}$ cm^{-3}
Emitter	$Al_{0.3}Ga_{0.7}As$ 0.181μm	N $5x10^{17}$ cm^{-3}
Base	GaAs 0.1μm	p^+ $1x10^{18}$ cm^{-3}
Collector\ Absorber	3 $In_{0.2}Ga_{0.8}As/GaAs$ 80Å/1300Å MQW	n^- $5x10^{16}$ cm^{-3}
Sub-Collector	GaAs 0.4175μm	n^+ $3x10^{18}$ cm^{-3}
Isolation	GaAs 0.42μm	undoped
Etch stop	$Al_{0.75}Ga_{0.25}As$ 0.29μm	undoped
P-contact	GaAs	p^+ $5x10^{18}$ cm^{-3}
Confinement Layer	$Al_{0.98}Ga_{0.02}As$ 240Å	p^+ $1x10^{18}$ cm^{-3}
λ/2 Cavity	Graded GaAs/AlAs superlattice	
	$In_{0.2}Ga_{0.8}As/GaAs$ 60Å/100Å QW	
	Graded GaAs/AlAs superlattice	
	x26 GaAs/AlAs 0.0696μm 0.0829μm DBR TOP 3 pairs n^+ $2x10^{18}$ cm^{-3}	
	SI Substrate and buffer GaAs	

(b)

Fig. 1. (a) Equivalent circuit and (b) heterostructure for integrated HPT/MCLED (VCSEL) phototransceiver, grown by molecular-beam epitaxy.

VCSEL. The main function of the OEIC is to detect, amplify, and retransmit optical signals with high gain, low noise, high resolution, and minimum power consumption. The input and output light wavelengths can also be different, if necessary. The equivalent circuit of the OEIC is shown in Fig. 1(a). In the circuit, a vertical integration scheme, with an isolation layer, is adopted in which the heterostructure of each device is independently optimized. This approach provides advantages of one-step epitaxy, simpler fabrication, and higher yield.

The heterostructure shown in Fig. 1(b) was grown, in a single step, by molecular-beam epitaxy. The VCSEL/MCLED, which is first grown, utilizes 23 periods of undoped GaAs/AlAs and three periods of n-doped (5×10^{18} cm^{-3}) $GaAs/Al_{0.8}Ga_{0.2}As$ distributed Bragg reflector (DBR) mirror grown on a semi-insulating GaAs substrate. Only the top three periods are doped in order to reduce free carrier absorption, which might affect the threshold current of the laser and the efficiency of the MCLED. The active region consists of a single $In_{0.2}Ga_{0.8}As/GaAs$ quantum well that emits light at 980 nm. The thickness of the barrier and well regions is 100 and 60 Å, respectively. Two undoped graded superlattice spacer layers are used to sandwich the quantum-well region and form the $\lambda/2$ cavity. A 24-nm $Al_{0.98}Ga_{0.02}As$ layer is grown on top of the cavity layer to provide current confinement after lateral wet oxidation of the layer. A quarter-wave layer of p^+ GaAs is grown on top of the cavity and forms the top contact layer. This heterostructure

essentially forms the MCLED. To realize a VCSEL, six pairs of MgF/ZnSe are deposited to form the top DBR mirror.

The performance of an HPT is usually determined by its responsivity and quantum efficiency. For massively parallel applications, high values of f_T and f_{max} are not required. The MQW-HPT consists of a 4175 Å n^+ (3×10^{18} cm^{-3}) GaAs subcollector layer, a 1000 Å p^+ (1×10^{18} cm^{-3}) GaAs base, a 1810 Å n (5×10^{17} cm^{-3}) $Al_{0.3}Ga_{0.7}As$ emitter, an 890 Å n^+ (3×10^{18} cm^{-3}) $Al_{0.3}Ga_{0.7}As$ subemitter, and a 1390 Å n (3×10^{18} cm^{-3}) GaAs contact layer. The collector/absorber layer consists of 3 $In_{0.2}Ga_{0.8}As/GaAs$ quantum wells (80-Å well and 1300-Å barrier). The layers are designed such that the MQWs are placed at the maxima of the optical field distribution of the incident light. The quantum-well absorption peak occurs at 980 nm, which coincides with the resonant frequency of the bottom DBR mirror. Our objective was to compare the performance of the phototransceiver with 850- and 980-nm light, where a partially resonant cavity with the bottom DBR is formed. As will be evident later, we have characterized the phototransceiver with both 850- (GaAs) and 980-nm (MQW) input photoexcitation. The HPT heterostructure is separated from the MCLED by a 0.29 μm $Al_{0.7}Ga_{0.3}As$ etch-stop layer and a 0.42 μm GaAs layer. The purpose of these undoped layers is to facilitate the fabrication process and to electrically isolate the HPT from the MCLED. To increase the optical gain of the HPT, the base transit time should be minimized and the electron mobility should be maximized. Based on this, the base region is chosen to have a thickness of 100 nm and a doping of 10^{18} cm^{-3} (doped with Be). The low base doping also helps to prevent outdiffusion, which may occur during the epitaxy, processing, and circuit operation and result in possible junction displacement toward the emitter, away from the $GaAs/Al_{0.3}Ga_{0.7}As$ heterojunction. Such displacement would introduce parasitic homojunction effects and results in a reduction in the current gain and the optical gain of the circuit. To ensure minimal outdiffusion of Be, the base and emitter layers are grown at 560 °C, and the rest of the heterostructure is grown at 600 °C.

B. Circuit Fabrication

The OEIC is fabricated by standard photolithography and liftoff techniques and a combination of dry and selective wet etching. The fabrication procedure is as follows: the HPT layers, above the MCLED (or VCSEL), are selectively etched away in order to expose the MCLED p-contact layer. A combination of dry and wet etch are used. The MCLED mesa is then formed by etching in a mixture of BCl_3 and Ar gases, followed by etching in $H_3PO_4 : H_2O_2 : H_2O$ (1:1:30), to remove any damage that may have resulted from the reactive ion etching (RIE). The sample then undergoes cleaning in an oxygen plasma, followed by a long clean in hot photoresist stripper (PR1000) prior to oxidation. The sample is then oxidized in a clean horizontal tube furnace at 450 °C in a water vapor ambient. The exposed $Al_{0.98}Ga_{0.02}As$ layer is laterally oxidized to form the desired active area size. The lateral oxidation rate of $Al_{0.98}Ga_{0.02}As$ at 450 °C is ~ 2 μm/min. This is followed by p-ohmic (Pd/Zn/Pd/Au = 100/100/200/2000 Å), and n-ohmic (Ni/Ge/Au/Ti/Au = 250/325/650/200/2000 Å) contact formation. The emitter mesa of the HPT is then delineated using a combination of RIE and wet etching. The collector contact metal is next deposited and the devices are isolated. The HPT and the MCLED/VCSEL are planarized by polyimide deposition. Interconnection metal (Ti/Al/Ti/Au) with 1.5 μm thickness is then evaporated. The emitter cap GaAs layer on top of the HPT is next removed by wet etch. If the light emitter in the OEIC is intended to be a VCSEL, then six pairs of 1790-Å MgF/830 Å ZnSe are selectively deposited to from the top mirror. The schematic and photomicrograph of the phototransceiver are shown in Fig. 2(a) and (b), respectively.

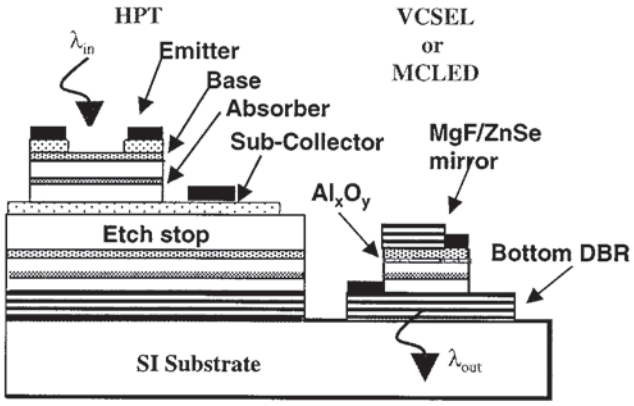

(a)

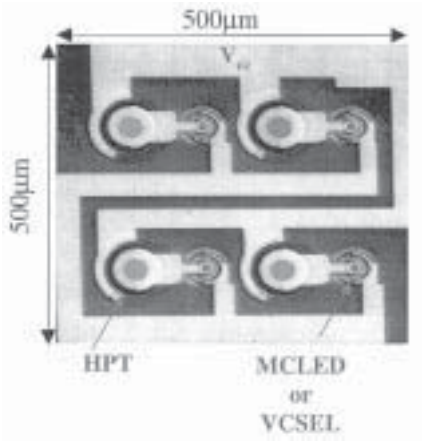

(b)

Fig. 2. (a) Schematic cross-section of the GaAs-based phototransceiver OEIC. (b) Scanning electron photomicrograph of a 2 × 2 array of the integrated phototransceiver.

III. Devices and Circuit Characteristics

A. MCLED and VCSEL Characteristics

The main advantage of VCSELs for this application is that they have low threshold current ($\sim$ 100 μA) and can provide very high quantum efficiency. Unfortunately, to provide a high efficiency, the VCSEL should be operated well above I_{th}, which enhances the circuit power dissipation. In order to maintain the power dissipation of the circuit at 500 μW (or less), the integration of HPT with a MCLED might be more appropriate. To ascertain whether the VCSEL or the MCLED is more suitable for the operation of the OEIC, we have compared their output characteristics. It may be remembered that both devices

are made from the same heterostructure. An additional top MgF/ZnSe DBR provides VCSEL characteristics. The devices tested have 3 μm apertures defined by lateral wet oxidation of the $Al_{0.98}Ga_{0.02}As$ layer. As can be seen in Fig. 3, the MCLED has $\sim 7\%$ differential quantum efficiency for a wide range of operating currents (< 400 μA). On the other hand, the VCSEL, with six pairs of MgF/ZnSe, has a threshold current of 90 μA and $\sim 35\%$ quantum efficiency. The results imply that in the phototransceiver, the VCSEL can provide higher optical gain (by a factor of five) than the MCLED. It should be noted that the difference in gain can be compensated by redesigning the HPT to attain higher optical gain (responsivity) in the MCLED. From the data shown in Fig. 3, it can be concluded that for low power dissipation, a phototransceiver circuit can be realized with a high-efficiency MCLED. The peak output wavelengths of the VCSEL and MCLED are 985 and 980 nm, respectively.

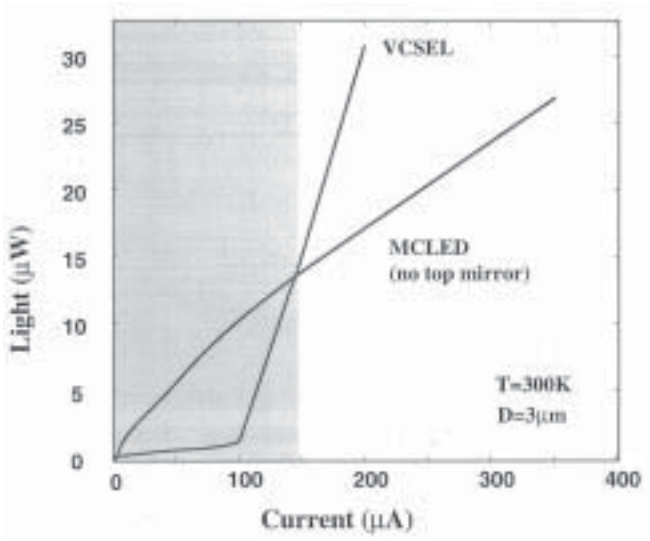

Fig. 3. Light–current characteristics of 3 μm aperture oxide-confined MCLED and VCSEL. The laser contains six periods of MgF/ZnSe top DBR mirror.

B. Phototransistor Characteristics

The optical gain (or responsivity) of the phototransistor, which is considered as an important performance characteristic, is determined by factors such as carrier recombination in the neutral and space-charge regions and surface recombination. The fabricated MQW-HPTs have a diameter of 85 μm and window opening of 35 μm. The devices have low dark current ($\sim$ 2 nA) and reasonably high breakdown voltage (> 5V). The offset voltage is very close to zero, indicating symmetric BE and BC junctions. The optical gain and DC characteristics of the fabricated MQW-HPTs, without antireflection coating, were measured using 850- and 980-nm lasers, a tapered optical probe, and HP4145 parameter analyzer. The responsivity of the HPT was determined by measuring the photogenerated current as a function of incident optical power. The responsivity and the photocurrent of the HPT as a function of input power (850 nm) are shown in Fig. 4(a). As observed from the measured data, the device exhibits high optical gain at low input power ($G > 60$ A/W at $P_{\text{in}} = 1$ μW). The responsivity can be increased, at least by a factor of 1.3, with the incorporation of an antireflection (AR) coating on the top surface. Shown for comparison, in Fig. 4(b), is the responsivity with 980-nm photoexcitation. It is interesting to note that the two responsivity curves are comparable. We believe that the small absorption in only three quantum wells is compensated by the resonance effect at 980 nm provided by the bottom DBR. Because of this similarity in the responsivity characteristics of the HPT, the phototransceiver circuits were characterized with only 850-nm light.

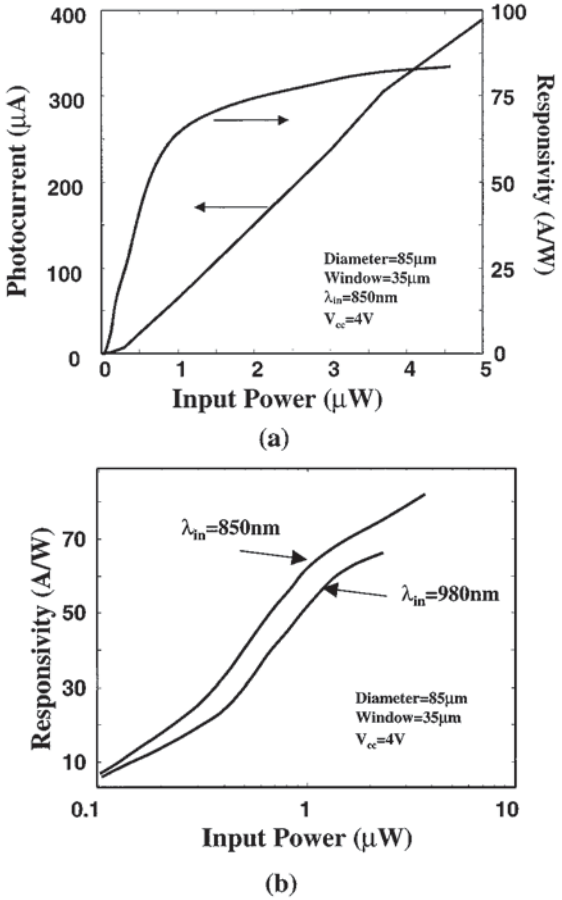

Fig. 4. (a) Photocurrent and responsivity of MQW-HPT as a function of incident optical power ($\lambda = 850$ nm). (b) Responsivity of the phototransistor for 850- and 980-nm photoexcitation light.

C. Phototransceiver Characteristics

Fig. 2(b) shows the scanning electron photomicrograph of one pixel, consisting of four phototransceivers. The pixel size is 500×500 μm^2. The relatively large pixel size is used here in order to facilitate the circuit characterization. The optical input–output characteristics of the monolithically integrated circuits were measured using a GaAs laser, a tapered optical probe, and a Ge detector. The measured input-output characteristics ($\lambda_{\text{in}} = 850$ nm and $\lambda_{\text{out}} = 980$ nm) of the VCSEL and MCLED-based monolithically integrated circuits, without AR coating, are shown in Fig. 5. The figure also shows, for comparison, the calculated input–output characteristics of the OEICs using computer-aided design tools (MEDICI). Both circuits show excellent characteristics at low input power.

The optical gain of the OEIC is a function of input power (i.e., photocurrent), which originates from the dependence of the

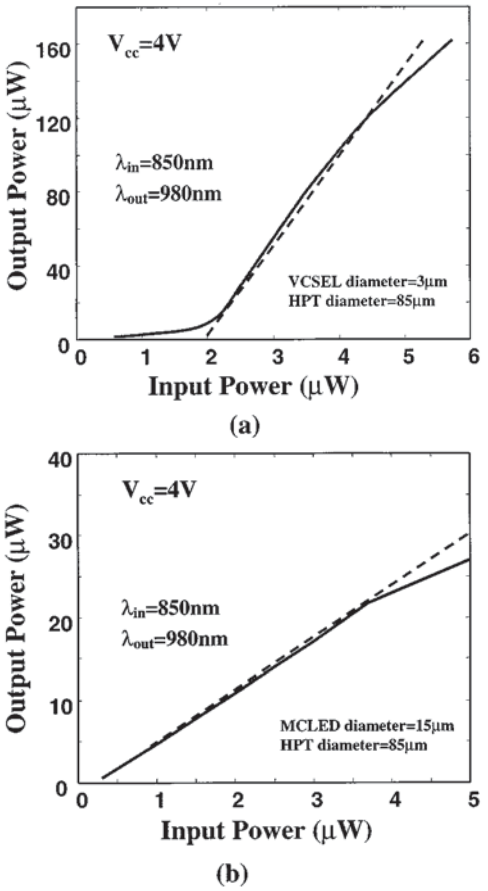

Fig. 5. Optical input–output characteristics of the monolithically integrated phototransceiver circuit: (a) incorporating a VCSEL and (b) incorporating an MCLED. The dashed lines indicate calculated results.

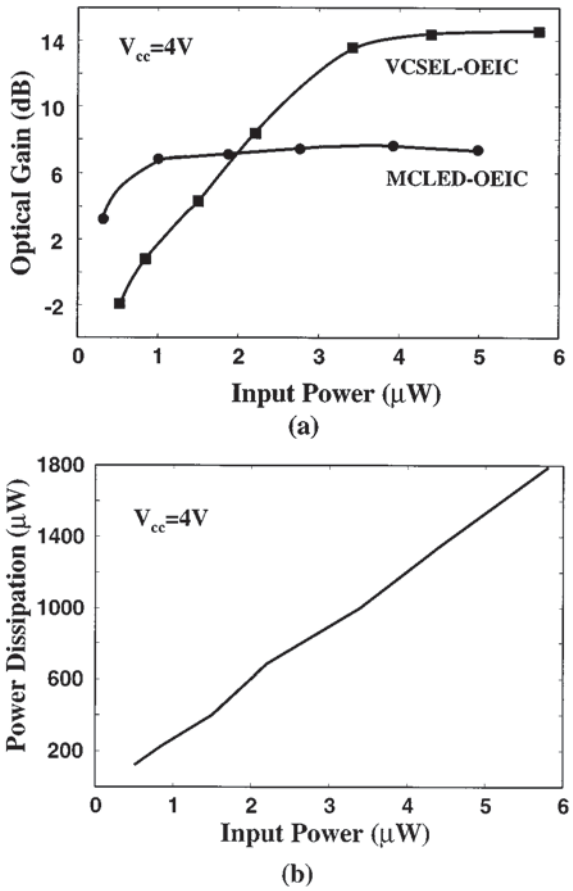

Fig. 6. (a) Optical gain of the OEICs as a function of input power and (b) power dissipation as a function of input power.

current gain (β) of the HPT on the collector current. The optical gain of the phototransceiver, neglecting surface recombination, can be expressed as

$$G = \left[\frac{I_c}{I_{scr} + I_{rb}}\right] \eta_p \eta_o \frac{h\nu}{q} = \left[\frac{\beta_{max}}{1 + \kappa I_c^{-1+1/n}}\right] \eta_p \eta_o \frac{h\nu}{q} \quad (1)$$

where

- η_o differential quantum efficiency of the MCLED or VCSEL;
- η_p quantum efficiency of the HPT;
- I_{scr} recombination current in the base-emitter space charge region;
- I_{rb} recombination current in the neutral base region;
- I_c collector photocurrent;
- β_{max} I_c/I_{rb};
- n ideality factor of the phototransistor;
- q electron charge;
- $h\nu$ light energy;
- κ constant derived from the ratio of I_{scr}/I_{rb}.

At low current, $G \sim I^{1-1/n}$; and at high current, $G \sim \beta_{max}$. The ideality factor of the MQW-HPT is estimated to be 1.3 from the current gain of the phototransistor. The measured optical gain and power dissipation of the OEICs are shown in Fig. 6. As can be seen in the figures, the VCSEL-based OEIC exhibits an optical gain of 10 dB at an input power of 2.5 μW. The corresponding power dissipation of the circuit is 760 μW. On the other hand, the MCLED-based circuit demonstrates higher optical gain than the VCSEL-based circuit at input powers less than 2 μW. At $P_{in} = 1.5$ μW, the MCLED-based circuit exhibits an optical gain of ~ 7 dB. The total power consumption of the circuit at this input power is 400 μW. The optical gain of the MCLED-based circuit can be further increased by using AR coating on the HPT and optimization of device parameters (base doping and thickness of MQW-HPT and optical confinement factor of MCLED). It is evident that the MCLED-based OEIC demonstrates low power dissipation and high optical gain, which are necessary for the envisioned application.

It is important to consider the noise performance of the circuit. With the MCLED as the light emitter, shot noise in the HPT and the LED is the dominant source of noise. It should be noted that unlike an avalanche photodiode, the HPT has less excess noise associated with the gain process. The power signal-to-noise ratio of the circuit is given as shown in (2) at the top of the next page [18], where

- P_{in} input power;
- I total current consisting of photocurrent and dark currents;
- β frequency-dependent current gain;
- h_{FE} common emitter current gain;
- k Boltzmann constant;

$$\frac{S}{N} = \frac{1/2(q\eta_{\rm p}(P_{\rm in}/h\nu))^2(\beta+1)^2}{2qBI(h_{\rm FE}+1)[1+2\beta(\beta+1)/(h_{\rm FE}+1)]+4kT(B/R_{\rm s})+\overline{i_{\rm m}^2}} \tag{2}$$

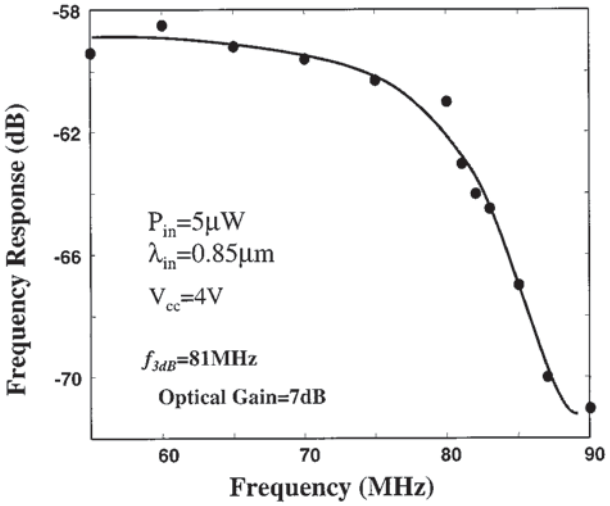

Fig. 7. Frequency response of an HPT-MCLED phototransceiver.

T effective noise temperature;

$R_{\rm s}$ load resistance associated with the MCLED;

B effective bandwidth of the circuit;

$\overline{i_{\rm m}^2}$ mean square noise current due to shot noise in the MCLED.

The calculated signal-to-noise ratio of the OEIC at $P_{\rm in} = 0.1\ \mu$W is $\sim$ 19 dB.

The frequency response of an HPT-MCLED phototransceiver was measured using a high-speed single-mode edge-emitting GaAs laser ($\lambda = 880$ nm) and HP8593A spectrum analyzer. The laser was modulated with an HP8350 sweeper oscillator and coupled onto a single-mode fiber. The modulated light was focused onto the HPT with a tapered optical probe, and the optical response of MCLED was measured by a high-speed photodiode low-noise amplifier, and spectrum analyzer. The frequency response of the monolithically integrated circuit is shown in Fig. 7. The measured bandwidth of the photoreceiver, which is limited by the RC time constant of the HPT, was 80 MHz.

IV. Conclusion

Two low-power GaAs-based monolithically integrated phototransceiver circuits have been designed, fabricated, and characterized. The first phototransceiver, consisting of a low-threshold VCSEL and a high-gain phototransistor, demonstrates an optical gain of 10 dB and power consumption of 760 μW at an input power of 2.5 μW. The second circuit, consisting of a high-efficiency MCLED and a high-gain phototransistor, demonstrates an optical gain of 7 dB and power consumption of 400 μW at an input power of 1.5 μW. The MCLED-based circuit exhibits a small signal modulation bandwidth of 80 MHz, limited by the RC time constant of the circuit. It is evident that the OEICs demonstrate low power dissipation and high optical gain, which are required for highly parallel imaging and sensing applications.

References

[1] E. Fossum, "CMOS image sensors: Electronic camera-on-a-chip," *IEEE Trans. Electron Devices*, vol. 44, pp. 1689–1698, 1997.

[2] K. Itakura, T. Nobusada, Y. Toyoda, Y. Saitou, N. Kokusenya, R. Nagayoshi, M. Ozaki, Y. Sugawara, K. Mitani, and Y. Fujita, "A 2/3-in 2.0 M-pixel CCD imager with an advanced M-FIT architecture capable of progressive scan," *IEEE Trans. Electron Devices*, vol. 44, pp. 1625–1632, 1997.

[3] J. Lavine and E. Banghart, "The effect of potential obstacles on charge transfer in image sensors," *IEEE Trans. Electron Devices*, vol. 44, pp. 1593–1598, 1997.

[4] E. Fossum, "Low power camera-on-a-chip using CMOS active pixel sensor technology," in *Proc. 1995 IEEE Symp. Low Power Electronics*, San Jose, CA, Oct. 1995, pp. 8–10.

[5] K. Beyzavi, D. Kim, C. Chao, P. Burrows, and S. Forrest, "A cascadable InGaAsP-InP optoelectronic smart pixel with low switching energy," *IEEE Photon. Technol. Lett.*, vol. 7, pp. 1162–1164, 1995.

[6] A. Alduino, G. Ortiz, C. Hains, B. Lu, Y. Lu, J. Cheng, R. Schneider, J. Klem, and J. Zolper, "500 Mbit/s operation of a multifunctional binary optical switching fabric," *Electron. Lett.*, vol. 31, pp. 1570–1571, 1995.

[7] Y. Lu, J. Cheng, J. Zolper, and J. Klem, "Integrated optical/optoelectronic switch for parallel optical interconnects," *Electron. Lett.*, vol. 31, pp. 579–581, 1995.

[8] J. Cheng, P. Zhou, S. Sun, S. Hersee, D. Myers, J. Zolper, and G. Vawter, "Surface-emitting laser-based smart pixels for two-dimensional optical logic and reconfigurable optical interconnects," *IEEE J. Quantum Electron.*, vol. 29, pp. 741–756, 1993.

[9] D. Deppe, D. Huffaker, T. Oh, H. Deng, and Q. Deng, "Low-threshold vertical-cavity surface-emitting lasers based on oxide-confinement and high contrast distributed Bragg reflectors," *IEEE J. Select. Topics Quantum Electron.*, vol. 3, pp. 893–904, 1997.

[10] Z. Zou, D. Huffaker, and D. Deppe, "Ultralow-threshold cryogenic vertical-cavity surface-emitting laser," *IEEE Photon Technol. Lett.*, vol. 12, pp. 1–3, 2000.

[11] D. Huffaker and D. Deppe, "Intracavity contacts for low-threshold oxide-confined vertical-cavity surface-emitting lasers," *IEEE Photon Technol. Lett.*, vol. 11, pp. 934–936, 1999.

[12] ——, "Low threshold vertical-cavity surface-emitting lasers based on high contrast distributed Bragg reflectors," *Appl. Phys. Lett.*, vol. 70, pp. 1781–1783, 1997.

[13] J. Blondelle, H. Neve, P. Demeester, P. Daele, G. Borghs, and R. Baets, "16% external quantum efficiency from planar microcavity LED's at 940 nm by precise matching of cavity wavelength," *Electron. Lett.*, vol. 31, pp. 1286–1288, 1995.

[14] J. Wierer, D. Kellogg, and N. Holonyak, "Tunnel contact junction native-oxide aperture and mirror vertical-cavity surface-emitting lasers and resonant-cavity light-emitting diodes," *Appl. Phys. Lett.*, vol. 74, pp. 926–928, 1999.

[15] L. Graham, D. Huffaker, and D. Deppe, "Spontaneous lifetime control in a native-oxide-apertured microcavity," *Appl. Phys. Lett.*, vol. 74, pp. 2408–2410, 1999.

[16] H. Neve, J. Blondelle, P. Daele, P. Demeester, and R. Baets, "Recycling of guided mode light emission in planar microcavity light emitting diodes," *Appl. Phys. Lett.*, vol. 70, pp. 799–801, 1997.

[17] H. Neve, J. Blondelle, R. Baets, P. Demeester, P. Daele, and G. Borghs, "High efficiency planar microcavity LED's: Comparison of design and experiment," *IEEE Photon. Technol. Lett.*, vol. 7, pp. 287–289, 1995.

[18] R. Milano, P. Dapkus, and G. Stillman, "An analysis of the performance of heterojunction phototransistors for fiber optic communications," *IEEE Trans. Electron. Devices*, vol. ED-29, pp. 266–273, 1982.

Omar Qasaimeh (M'00) received the B.S. and M.S. degrees in electrical engineering from Jordan University of Science and Technology, Irbid, Jordan, in 1992 and 1994, respectively, and the Ph.D. degree in electrical engineering from the University of Michigan, Ann Arbor, in 2000.

His research interests include design, fabrication, characterization, and development of high efficiency, high-speed optoelectronic devices and integrated circuits. He is currently working on the development of tunable lasers at Agere systems (formerly Lucent Technologies), Breinigsville, PA.

Weidong Zhou (S'00), photograph and biography not available at the time of publication.

Pallab Bhattacharya (M'78–M'83–F'89), photograph and biography not available at the time of publication.

Diana Huffaker (M'96), photograph and biography not available at the time of publication.

Dennis G. Deppe (S'85–M'90–SM'97–F'00), photograph and biography not available at the time of publication.